20

A simple optical scanner for transmission imaging of biological objects

© A. Khanbekyan, S. Shmavonyan, P. Saakyan, H. Sultanyan, M. Movsisyan, A. Papoyan

Institute for Physical Research, National Academy of Sciences of Armenia,
Ashtarak-2, Armenia

e-mail: akhanbekyan@gmail.com

Received August 23, 2024
Revised September 22, 2024
Accepted September 27, 2024

A scheme of a transmission imaging setup for biomedical applications is presented, based on point-by-point spatial scanning of a continuous-wave laser beam and preferential registration of transmitted ballistic photons. A special feature of the scheme is the simplicity of microcomputer control of scanning modes and processing of the recorded signal, as well as the use of an inexpensive, highly sensitive photodetector with an extended dynamic range and high linearity of response. The performance of the scheme was tested on model and biological objects.

Keywords: optical imaging, ballistic photons, point-by-point scanning, visualization of biological objects.

DOI: 10.61011/EOS.2024.09.60048.7013-24

Introduction

Optical virtualization of highly scattering and absorbing media continues attracting the researchers' attention as a potential mechanism for non-destructive diagnostics. Of particular interest is the visualization of biological tissues, organs and structures, where the use of diagnostic procedures associated with ionizing and coagulating effects, reversible and irreversible changes in the physiological state is highly undesirable.

Optical visualization is minimally invasive, while at the same time, the effective depth of light penetration into biological tissues, especially *in vivo*, is extremely low, primarily due to multiple scattering caused by inhomogeneities of biological tissues and resulting in severe image distortion [1]. To minimize the scattering effect the methods of adaptive optics [1], diffuse optical tomography [2] and optical coherence tomography [3], optical heterodyne detection [4], in particular, as well as other methods are used. The expediency of using a particular method depends on the optical properties of the biological sample under study [5].

The promising approach is the selective recording of the so-called „ballistic" photons — a small portion of light passing through the examined object without scattering (i.e. without changing the direction). Such light can be selected by a temporary gate when an object is illuminated with femtosecond radiation: the photons that are not scattered are the first to reach the photodetector [6]. Ballistic photons can also be selected spatially. e.g. by limiting the solid angle of recording [7]. Recently, single-photon avalanche diode (SPAD) arrays have been successfully used to visualize ballistic photons, allowing single photons to be recorded while providing the necessary temporal resolution [8].

The aim of this study was to develop a simple and inexpensive visualization system by method of transmission imaging for biomedical applications based on a point-by-point scanning with a continuous laser beam and recording of radiation transmitted in the same direction by a single photodetector [9,10]. The advantage of this approach is the facilitated processing of the recorded signal (averaging, demodulation, filtering, etc.). The specifics of this study is the geometric configuration of the measuring system, which mainly records ballistic light and cuts off scattered light, as well as the use of a highly sensitive photodetector with an extended dynamic range and highly linear response.

Schematic representation of scanner

The device consists of mechanical part and electronic control and recording unit (Fig. 1). The source of collimated laser radiation (*1*) and the photodetector (*2*) axially aligned on a movable frame (*5*) are moving in the horizontal plane XY. Scanning along a given trajectory with a given increment is carried out by means of the two stepper motors. The motion distance in both directions is 60 mm with an error of 0.1 mm.

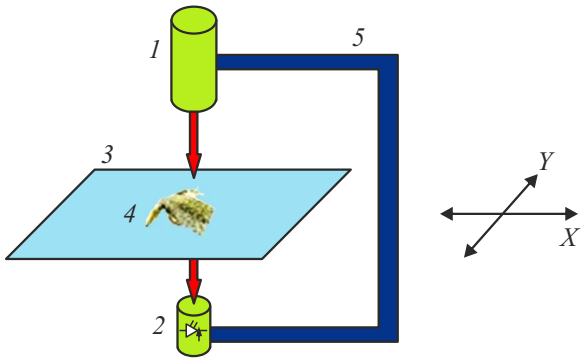

Figure 1. Schematic representation of scanner: *1* — laser source, *2* — photoreceiver, *3* — object glass holder, *4* — examined object, *5* — two-layer movable frame with the stepper motors.

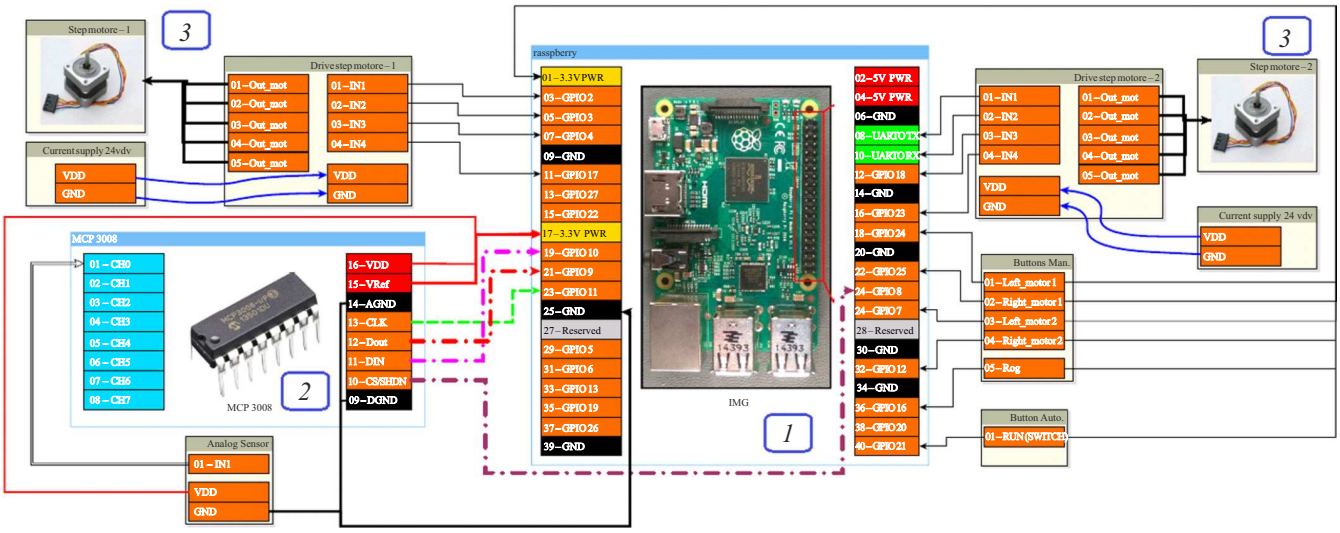

Figure 2. Electrical diagram of scanner. *1* — Raspberry Pi3 microcomputer, *2* — analog-to-digital converter MCP3008, *3* — stepper motors.

The examined sample (*4*) is placed on a steady object glass holder (*3*), installed in a space between the laser source and photodetector. The choice of the laser radiation wavelength is determined by the specific purpose of the research. In this study a continuous laser diode was used with a wavelength of 850 nm, fitting the first transparency window of biological tissues in the near infrared band (NIR-I, 700–950 nm, the so-called „therapeutic window“ [11]). The power of laser radiation was 50 mW with a diameter of collimated beam of 1 mm.

The laser radiation passing through the object under study was recorded by the OPT101 photodetector, which is a monolithic photodiode with a built-in operational transimpedance amplifier. The photodetector has a linear response in a wide dynamic range (10^5) with maximal optical sensitivity of 6 V/μW at a wavelength of 850 nm with resistance of the feedback resistor of $R_F = 10\,\text{M}\Omega$. Due to a monolithic structure maximum protection from external electrical interference is provided.

High sensitivity of the photodetector makes it possible to provide a working mode when only ballistic photons are predominantly recorded. With an area of the photodiode 5.2 mm^2 and distance between the object glass holder and photodiode of 50 mm the solid angle of recording makes 2 msr. To cut off the diffusely scattered lateral light, the detected light passes through a blackened lens hood installed in front of the photodetector. The lens hood also helps to remove the room lighting.

Electrical diagram of the scanner is shown in Fig. 2. Its central element is Raspberry Pi3 model B single-board microcomputer, equipped with a quad-core processor 1200 MHz, which provides the operation of the entire system. The stepper motors *X* and *Y* with appropriate drivers control the movement of the two-dimensional frame with the laser source and the photodetector relative to the object glass holder with the examined object on it. A tailored Python program code allows setting the initial coordinates of the frame, the trajectory and the step of movement, selecting the speed and the required number of scanning steps in *X* and *Y* directions, and also ensures that the scanning system returns to its original position upon completion of the measurement cycle.

The output signal of the photodetector is sent to a 10-bit analog-to-digital converter MCP3008 and transmitted to the digital input of the microcomputer. At each point (pixel) of scanning, the same program registers the radiation signal that has passed through the examined object, averages it over a specified time interval, and saves the measurement results in csv format for its further processing. The scanning data is represented as a graphical image by means of program in LabView or Wolfram environment allowing also to form a user color scale to define the signal magnitude.

Testing of the scanning system on modelled and biological objects

The system was checked in several steps. First, the repeatability of successive visualization cycles of the model object and the accuracy of returning the movable frame to its original position with the scanning mode unchanged were tested. A plate with two slits 4 mm wide and a distance between them of 2.5 mm was used as a model object. After the first scanning and automatic return to the initial state, the second scanning showed a complete match of the coordinates of the images.

At the next stage, the scanner was tested using a modelled planar scattering/absorbing object, which was a metal disk 20 mm in diameter installed in a slot in the center of black high-density spongy polyurethane sheet with a thickness of 12 mm. Scanning was done in the region

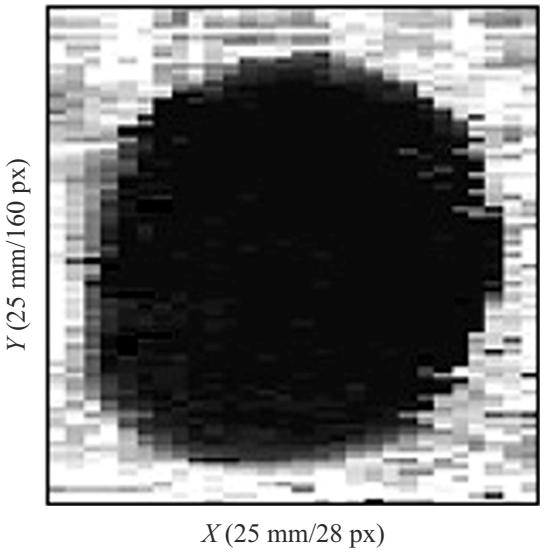

Figure 3. Scanned image of a metal disk 20 mm in diameter inserted into the high-density spongy polyurethane 12 mm thick.

25×25 mm, to determine the optimal step of scanning various numbers of pixels were selected for X and Y : 28 and 160 accordingly.

The scanning result in grayscale is shown in Fig. 3. It is clearly seen that a high-contrast image was obtained with a size corresponding to the original object with an error of no more than ± 0.5 mm in both X and Y. From this, it can be concluded that the image is formed mainly by ballistic photons, and reducing the scanning step much smaller than the diameter of the laser beam (1 mm) is impractical, since it does not lead to a higher spatial resolution.

A dried lizard of small size (length 50–60 mm) was studied as a simple biological object with variable thickness. A region of 20 mm in X and 40 mm in Y was scanned with a number of pixels 24 and 80, respectively. The result of scanning is shown in Fig. 4. It should be noted that due to the small thickness of the lizard's body, the transmission signal was high in the entire scanning area, and in the region of its legs with a thickness of 2–3 mm it exceeded the saturation threshold of the photodetector, therefore, the legs of the lizard did not appear in the image. Because of the small dynamic range of the signal for this object, a color scale of the image was applied for better visualization. Figure 4 clearly shows the internal structure of the lizard, expressed in dark (blue) tones.

The last object of the study was a human (one of the co-authors) finger. Scanning was done with an equal step of 0.7 mm in X and Y with the number of pixels 36 and 38, respectively. 10 consecutive measurements of the transmitted signal were carried out for each pixel (scanning point) and the average value was recorded. The color representation of the signal was carried out in grayscale (32 levels), and a logarithmic scale was used for better perception of the visualized image in conditions of highly varying signal strength. With a full dynamic range of a 10-bit full dynamic range of an analog-to-digital converter (1024 levels), the average ambient light level in a lighted room was 250.

The result of finger section scanning is shown in Fig. 5. The scanned region is marked with a rectangle on the left-side photo. Maximal thickness of the finger in the region of interphalangeal joint was 22 mm. A light-color lateral area is well observed on the scanned image. Obviously, it corresponds to the increased transparency of the joint capsule with synovial fluid and articular cartilage compared to the bones of the phalanges.

Discussion of the results

The above-mentioned results prove that the proposed method based on recording the ballistic photons with a single (monopixel) photodetector during spatial scanning with a collimated laser beam allows obtaining images of acceptable quality with optical transmission of both, planar model samples and biological objects of large (and variable) thickness. Let's compare the parameters of the images obtained using the proposed installation with the analogues described in the literature.

The closest to the proposed scheme is the method described in the work [7], where a wide parallel laser beam formed by a telescopic system at the optical waveguide output focuses on the examined object which is moved in transverse plane, and the transmitted radiation, entering a telescopic expander, focuses on a photodetector, thus ensuring selective recording of ballistic photons. With such configuration high spatial resolution is obtained ($\sim 25\,\mu$m), if only the thickness of the examined object is no larger than the waist area of the focused beam (~ 0.5 mm). The resolution in our method depends on the diameter of the collimated radiation beam (~ 1 mm), yet, the thickness of the studied sample may reach as high as ~ 20 mm.

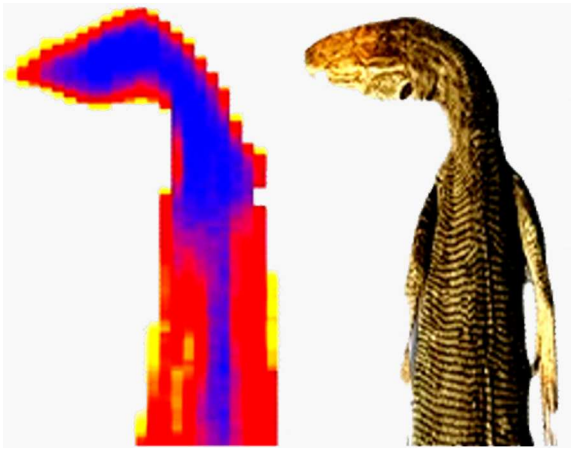

Figure 4. Scanned image (left) and photo (right) of a small dried lizard.

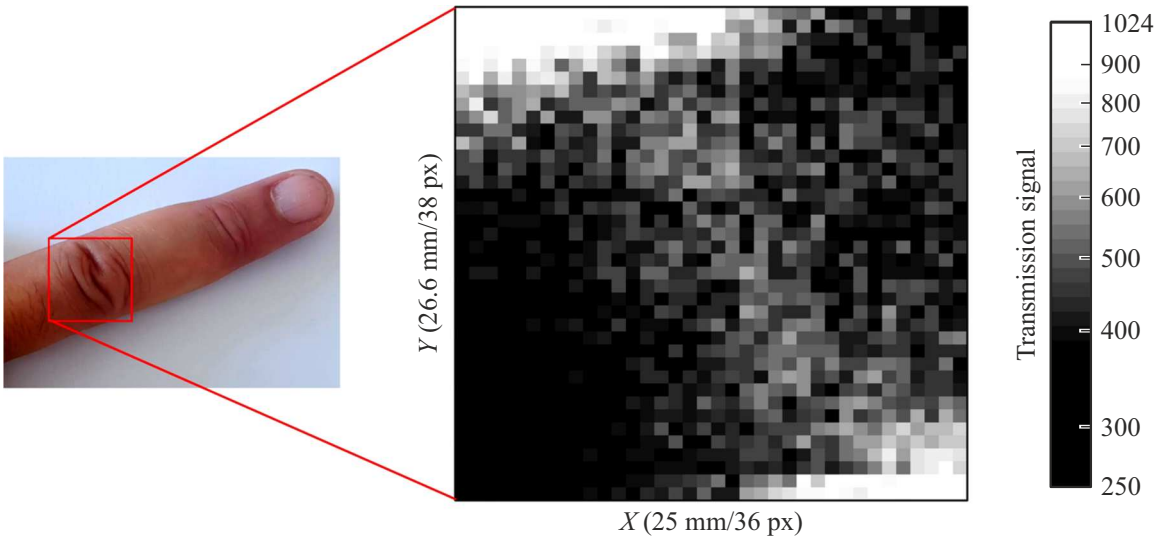

Figure 5. Scanned image of a section of the middle finger of a human's hand. The light area in the central part corresponds to the interphalangeal joint.

The ratio of maximum thickness of the examined object and spatial resolution is one of the main characteristics of visualization systems. A diagram representing this ratio for different visualization methods is given in the review paper [1]. It can be seen from this diagram that the greater the thickness of the examined object, the worse the resolution, while the method that provides the greatest penetration depth (thickness ~ 10 mm with a spatial resolution of 1 mm) is photoacoustic tomography based on generation of ultrasound from thermal expansion of the medium during optical energy absorption [12].

Summary and outlook

A device for optical transmission visualization of highly scattering objects, e.g., biological objects, has been developed and implemented. The device's operation principle is based on selective detection of transmitted ballistic photons by a highly sensitive photodetector during spatial scanning of the examined object with collimated laser radiation. Scanning and image recording are controlled by a software code installed in a single-board microcomputer.

It was demonstrated that the device may be used to visualize both, model objects and biological samples up to 20 mm thick (dried lizard, human finger joint). Predominant recording of ballistic photons with a minimal contribution of scattered light allows excluding necessity for a complex software processing of the obtained images.

The spatial resolution of the scanner in the absence of scattering is determined by the diameter of the collimated laser beam. It can be improved by installing a telescopic system that focuses the laser beam into the examined area, followed by the formation of a parallel beam of radiation directed at the photodetector.

It should be noted that in the proposed scheme, the contribution of scattered light to the image is suppressed, but not completely eliminated. In case of biological organs, the highest scattering occurs on the skin (epidermis), which the skin can be considered as a medium with a random but uniform distribution of scattering particles [13]: thus, the reduced scattering coefficient of the skin at a wavelength of 850nm is $\sim 12\,\text{cm}^{-1}$ [14]. To reduce this scattering, the use of biocompatible molecular agents promoting optical clearing of the skin [15] is implied in the future work.

Further improvement of the device also involves complete removal of external (background) illumination effect and increase of the image recording speed by optimizing the program and scanning trajectory.

Compliance with ethical standards

All procedures performed within the human subject research were in accordance with the ethical standards of the institutional and/or national research committee and with the 1964 Helsinki Declaration and later amendments or comparable ethical standards. Informed voluntary consent was obtained from each study participant.

Acknowledgments

The authors express their thanks to V.V. Tuchin for fruitful discussions.

Funding

The study was performed with the financial support of the Higher Education and Science Committee of the Republic of Armenia in the frame of the research project № 21AG1C082.

Conflict of interest

The authors declare that they have no conflict of interest.

References

[1] S. Yoon, M. Kim, M. Jang, Y. Choi, W. Choi, S. Kang, W. Choi. Nature Reviews Physics, **2**, 141–158 (2020). DOI: 10.1038/s42254-019-0143-2
[2] D. Lighter, J. Hughes, I. Styles, A. Filer, H. Dehghani. Biomedical Optics Express, **9**, 1445–1460 (2018). DOI: 10.1364/BOE.9.001445
[3] D.P. Popescu, L.P. Choo-Smith, C. Flueraru, Y. Mao, Sh. Chang, J. Disano, Sh.Sh. Sherif, M. Sowa. Biophys. Rev., **3**, 155–169 (2011). DOI: 10.1007/s12551-011-0054-7
[4] P. Zhan, W. Tan, J. Si, Sh. Xu, J. Tong, X. Hou. Appl. Phys. Lett., **104**, 211907 (2014). DOI: 10.1063/1.4880115
[5] I.S. Martins, H.F. Silva, E.N. Lazareva, N.V. Chernomyrdin, K.I. Zaytsev, L.M. Oliveira, V.V. Tuchin. Biomedical Optics Express, **14**, 249–298 (2023). DOI: 10.1364/BOE.479320
[6] J. Cho, S. Kang, B. Lee, J. Moon, Y.S. Lim, M. Jang, W. Choi. Optics Express, **29**, 35640–35650 (2021). DOI: 10.1364/OE.438443
[7] A.T. Mok, J. Shea, Ch. Wu, F. Xia, R. Tatarsky, N. Yapici, Ch. Xu. Biomedical Optics Express, **13**, 438–451 (2021). DOI: 10.1364/BOE.441844
[8] C. Bruschini, H. Homulle, I.M. Antolovic, S. Burri, E. Charbon. Light: Science & Appl., **8**, 87 (2019). DOI: 10.1038/s41377-019-0191-5
[9] K. Vardanyan, A. Khachaturova, S. Varzhapetyan, A. Badalyan, S. Shmavonyan, A. Papoyan. Optoelectronics and Advanced Materials — Rapid Commun., **4**, 1163–1165 (2010).
[10] K. Vardanyan, A. Khachaturova, S. Varzhapetyan, A. Badalyan, S. Shmavonyan, A. Papoyan. Proc. SPIE, **7998**, 799814 (2011). DOI: 10.1117/12.891718
[11] D. Sordillo, L. Sordillo, P. Sordillo, L. Shi, R. Alfano. J. Biomed. Opt., **22**, 045002 (2017). DOI: 10.1117/1.JBO.22.4.045002
[12] J. Xia, J. Yao, L.V. Wang. Progr. Electromagn. Res., **147**, 1–22 (2014). DOI: 10.2528/PIER14032303
[13] M.J.C. Van Gemert, S.L. Jacques, H.J.C.M. Sterenborg, W.M. Star. IEEE Transact. Biomed. Engineer., **36**, 1146–1154 (1989). DOI: 10.1109/10.42108
[14] H. Jonasson, I. Fredriksson, S. Bergstrand, C.J. Östgren, M. Larsson, T. Strömberg. J. Biomed. Opt., **23**, 121608 (2018). DOI: 10.1117/1.JBO.23.12.121608
[15] K.V. Berezin, K.N. Dvoretskii, M.L. Chernavina, V.V. Nechaev, A.M. Likhter, I.T. Shagautdinova, E.M. Antonova, V.V. Tuchin. Opt. Spectrosc., **127**, 352−358 (2019). DOI: 10.1134/S0030400X19080071

Translated by EgoTranslating